03,13

Structure and properties of composites based on aluminum and gallium nitrides grown on silicon of different orientations with a buffer layer of silicon carbide

© Sh.Sh. Sharofidinov[1,2], S.A. Kukushkin[2], M.V. Staritsyn[3], A.V. Solnyshkin[4], O.N. Sergeeva[4], E.Yu. Kaptelov[1], I.P. Pronin[1]

[1] Ioffe Institute,
St. Petersburg, Russia
[2] Institute of Problems of Mechanical Engineering, Russian Academy of Sciences,
St. Petersburg, Russia
[3] Central Research Institute of Structural Materials Prometey, National Research Centre Kurchatov Institute,
St. Petersburg, Russia
[4] Tver State University,
Tver, Russia

E-mail: sergey.a.kukushkin@gmail.com

Received December 30, 2021
Revised December 30, 2021
Accepted January 3, 2022

The microstructure and pyroelectric properties of $Al_xGa_{1-x}N$ composite epitaxial layers grown on SiC/Si(111) and SiC/Si(110) hybrid substrates by the chloride-hydride epitaxy have been studied. The phenomenon of spontaneous formation of a system of heterojunctions consisting of periodic $Al_xGa_{1-x}N$ layers of different composition located perpendicular to the direction of growth, was discovered during the growth of layers. Measurements of the pyroelectric coefficients of these heterostructures have shown that regardless of the orientation of the initial Si substrate and their pyroelectric coefficients have close values of the order of $\gamma \sim (0.7-1) \cdot 10^{-10}$ C/cm^{2}K. It is shown that to increase the magnitude of the pyroresponse it is necessary to deposit an AlN layer with a thickness exceeding $1\,\mu$m on the $Al_xGa_{1-x}N$/SiC/Si surface. This leads to record values of the pyroelectric coefficient $\gamma \sim 18 \cdot 10^{-10}$ C/cm^{2}K for AlN crystals and films.

Keywords: silicon carbide-on-silicon substrates, chloride-hydride epitaxy, AlGaN epitaxial layers, aluminum nitride, gallium nitride, pyroelectric properties.

DOI: 10.21883/PSS.2022.05.53510.250

1. Introduction

Wide-band nitride semiconductors (AlN, GaN, AlGaN) are the basic materials used in deep-UV photonics and high-performance photodetectors, LEDs and next-generation lasers [1–7]. For mass production of these devices, low-cost substrates, including silicon, are required. However, a great difference in the silicon and nitride lattice parameters hinders the use of silicon substrates. To overcome such difference, an atom substitution method was developed in [8–10] — formation of nanoscale silicon carbide buffer layers on a silicon substrate (SiC/(111)Si). Silicon carbide lattice parameters differ form those of hexagonal AlN by less than 1%. This made it possible to produce high quality epitaxial AlN layers on SiC/(111)Si substrates by the chloride-hydride epitaxy (CHE) method characterized by a high growth rate [11,12]. To obtain epitaxial GaN layers on such substrates, to reduce mechanical stresses and dislocations in them, it is reasonable to form $Al_xGa_{1-x}N$ solid solution transition layers [2–7,13]. It has been shown that the use of $Al_xGa_{1-x}N$ transition layers enables to produce GaN single crystals by the CHE method with a suitable crystalline quality and thickness of several hundred micron on SiC/(111)Si substrates with quality comparable with single-crystal layers produced by the CHE method during homoepitaxy on, „native" GaN substrates [14,15]. This makes it possible to expand the applications of wide-band nitride materials and in the nearest future begin to produce next-generation power electronics compatible with silicon electronics.

In addition, the polar axis, high spontaneous polarization and piezoelectric (electromechanical) parameters of aluminum and gallium nitrides make it possible to use them in the manufacture of a wide range of microelectromechanical transducers — from receiving and transmitting acoustic devices, actuators, sensors, etc., to various microwave-devices — generators, delay lines and filters that can function in a wide temperature range. By their electromechanical and pyroelectric properties, these materials are competitive with traditional ferroelectric materials such as lead zirconate-titanate solid solutions, lithium niobate and tantalate [16–23]. Polar properties of gallium and aluminum nitrides — $Al_xGa_{1-x}N$ with various ratios of Al and Ga have been scarcely studied until now. The interest in these materials can be explained

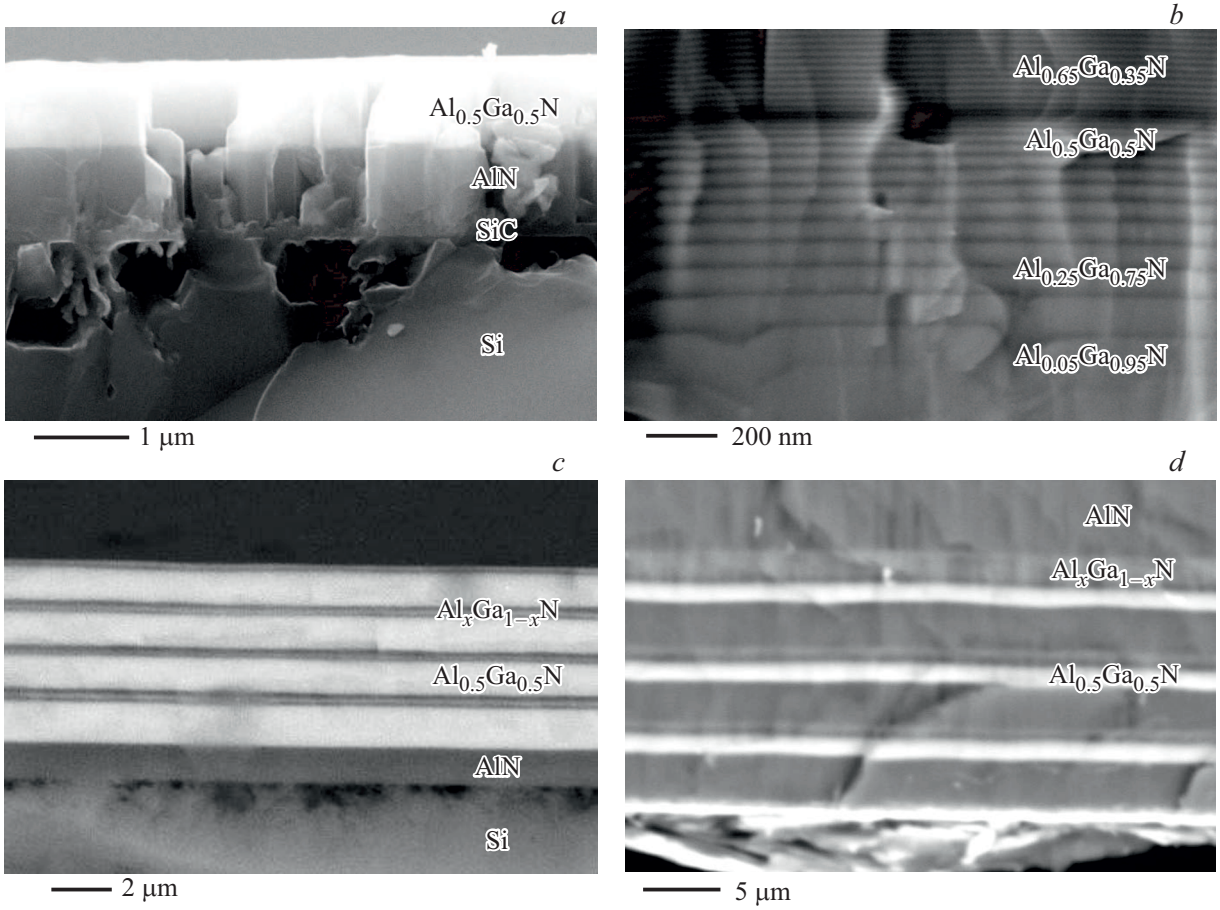

Figure 1. SEM images of end chipping in $Al_xGa_{1-x}N$ heterostructures formed on SiC/(110)Si (№ 1 and 2) and SiC/(111)Si (№ 3 and 4) substrates.

by the fact that they can combine high spontaneous polarization and electromechanical properties inherent in aluminum nitride with high pyroelectric parameters found in gallium nitride. Investigation of polar properties of such structures is hindered by their low-resistivity caused by high concentration of both point and extended structural defects.

In recent years, in addition to traditional heterostructure growing methods such as molecular beam epitaxy (MBE), metal-organic vapor phase epitaxy (MOVPE), sublimation growth, etc., extensive research has been carried out in the field of AlGaN epitaxial layer growth on SiC/Si substrates by the CHE method [24]. In the latter case, it is assumed that the use of substrates with another orientation may cause lower mechanical stresses in thin nitride layers and reduce the defect concentration. This, in turn, will allow to use epitaxial AlGaN layers to produce rather high-resistivity heterostructures to enable the study of their polar properties [25]. The purpose of the research was to investigate the relationship between the polar properties and microstructure and composition of heterostructures based on epitaxial AlGaN layers grown on nanoscale SiC surface formed by the matched atom substitution method [8–10] on silicon substrates with two orientations, i.e. on Si (111) surface and Si (110) surface.

2. Research methods and targets

For the research, several AlGaN heterostructures were selected that were grown by the CHE method on SiC/(111)Si and SiC/(110)Si substrates and suitable for dielectric and pyroelectric response measurements. The epitaxial AlGaN layer growth technique is described in [13,24]. In all cases the SiC buffer layer thickness was max. 90 nm.

Microstructural images of the surface and end chipping of AlGaN/SiC/Si(111) and AlGaN/SiC/Si(110) samples were obtained by the scanning electron microscopy (SEM) method using LIRA 3 (Tescan) system. To define the composition of heterostructures, an electron probe X-ray microanalysis method was used and implemented on X-Max EDS system (Oxford Instruments). The probe electron beam energy was equal to 12 keV. The crystalline structure of the samples was controlled by the X-ray diffraction analysis $\theta-2\theta$ (Rigaru, Ultima IV method). For electrophysical measurements, a platinum electrode was applied to the rear side of the silicon substrate and 1×1 mm platinum bonding

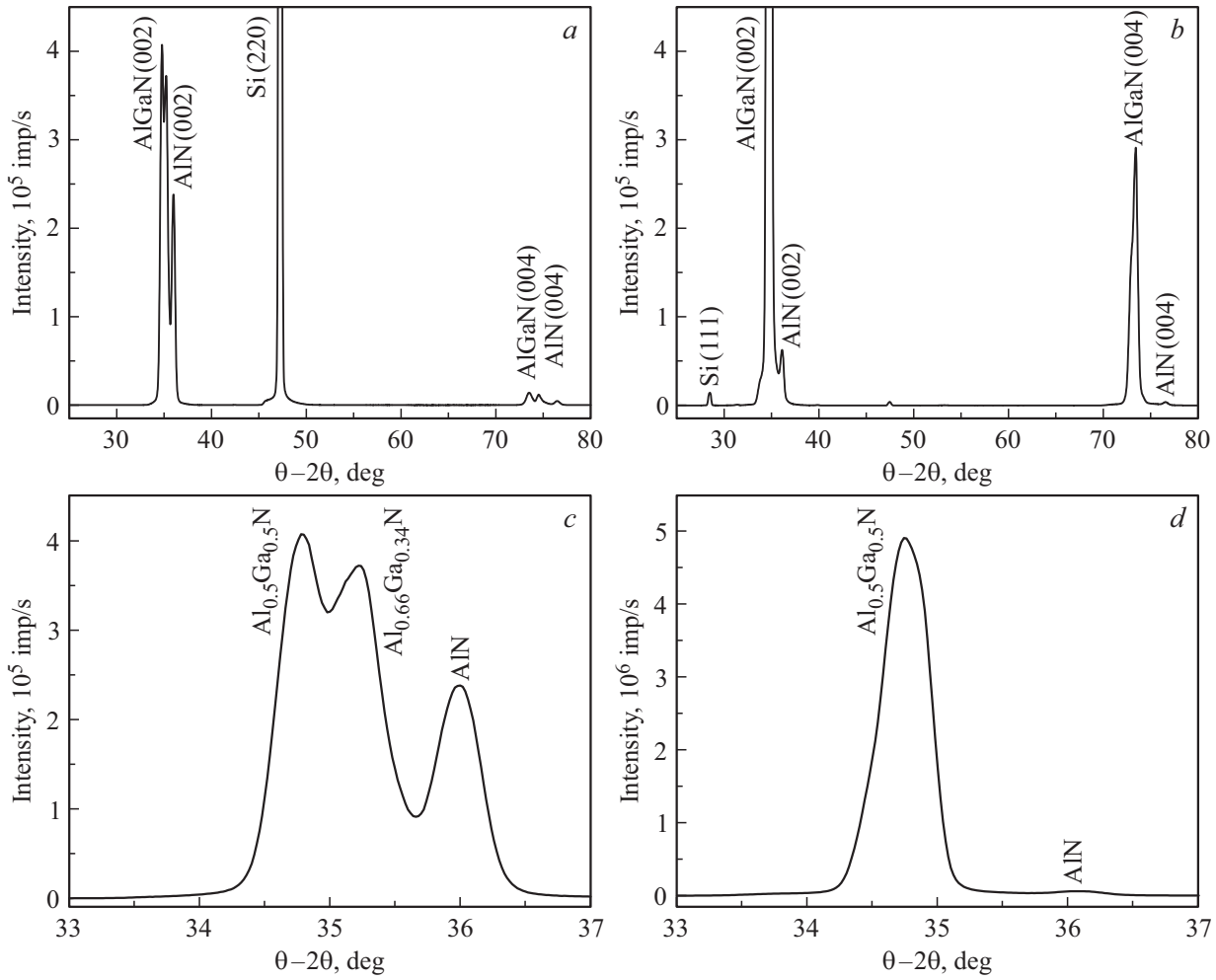

Figure 2. Diffraction patterns $\theta - 2\theta$ of AlGaN heterostructures (samples № 1 and 3) grown on SiC/(110)S (a, c) and SiC/(111)Si (b, d)substrates.

pads were formed on the heterostructure surfaces on the AlGaN side.

To induce dynamic pyroelectrical response, CLM-18451R-980 ($\lambda = 980$ nm) laser module was used with 220 mW heat flux modulated in the range from 1 Hz to 1000 Hz [23].

The first two samples (№ 1 and 2) were heterostructures grown on SiC/(110)Si substrate. Sample № 1 was a combination of consecutively grown AlN and AlGaN layers, $\sim 0.8\,\mu$m thick each (Fig. 1, a). Sample № 2 consisted of recurring AlGaN thin layers (70 nm and less) with variable composition. The composition varied from the substrate to the layer surface. Initially, an almost pure GaN layer was grown with GaN content of approx. 95 at.%. Then, with the increase in thickness, the layer was more and more enriched with Al. When a thickness of approx. 1.1 μm had been achieved, a sudden change in the layer composition occurred. This is clearly seen by the changed contrast (dark line) in Fig. 1, b. After this, Al become prevailing in the AlGaN layer. The uppermost layers were composed almost of pure AlN with low content of GaN.

The second group of samples (№ 3 and 4) was grown on SiC/(111)Si substrate. Sample № 3 was composed of several alternating AlGaN layers with various Al/Ga ratios and the total thickness of $\sim 7.3\,\mu$m (Fig. 1, c). Sample № 4 differed from the latter in that a thick ($\sim 200\,\mu$m) AlN layers was formed on the equivalent multilayer AlGaN structure (total thickness of $\sim 16\,\mu$m) (Fig. 1, d).

3. Experimental results and discussion

In accordance with the X-ray diffraction analysis data ($\theta - 2\theta$), the growth orientation of AlGaN heterostructures grown on SiC/(110)Si substrate corresponded to the hexagonal polar axis [002] (Fig. 2, a). In the selected diffraction pattern on sample № 1, the reflection located in $2\theta = 36°$ corresponded to the bottom layer with a composition close to aluminum nitride (Fig. 2, c). Two clearly distinguished reflections in the Figure correspond to the top AlGaN layer. They correspond to two AlGaN compositions — (1) Al/Ga = 0.50/0.50 and (2) Al/Ga $\approx$ 0.67/0.33. The AlGaN layer composition data defined by the reflection

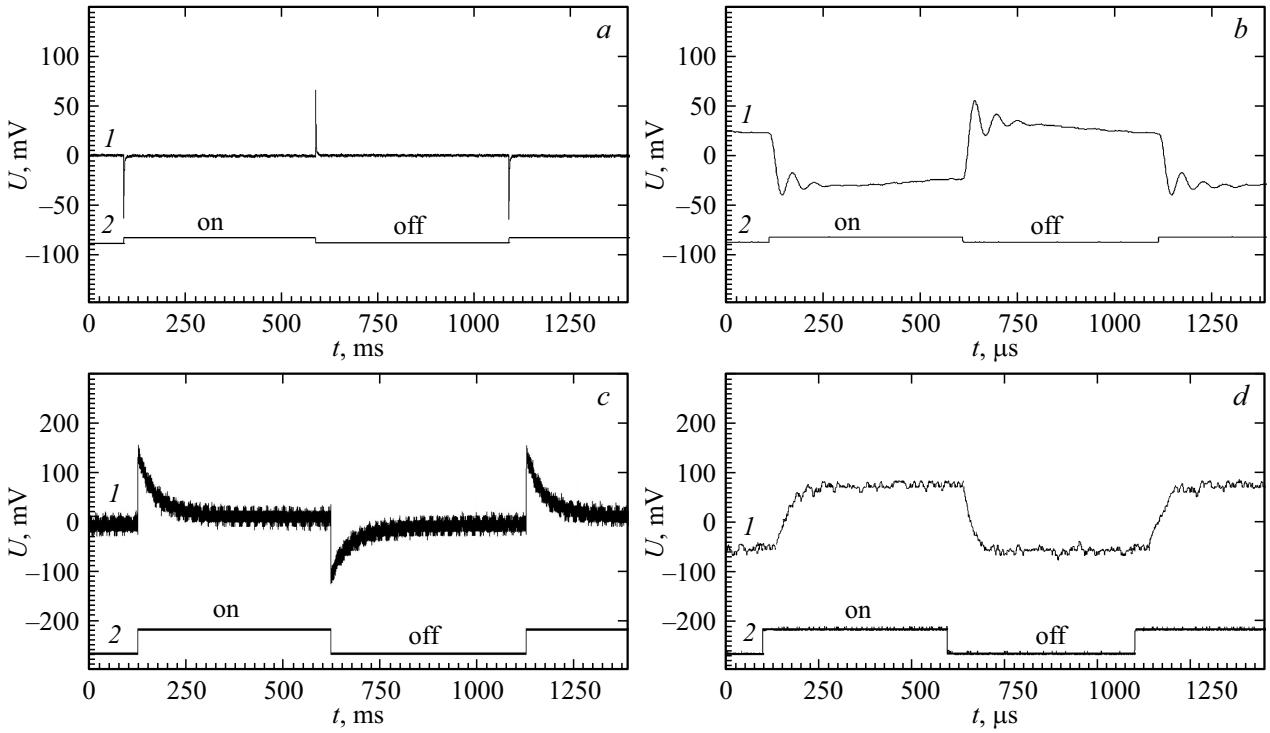

Figure 3. Pyroelectric response (curves *1*) of samples № 2 and 4 obtained at 1 Hz (*a, c*) and 1 kHz (*b, d*). Gates (2) illustrate the simulated heat flux.

positions on the diffraction pattern are well correlated with the data obtained by the electron probe X-ray microanalysis method. The SEM images of the sample surface have shown that there were two types of regions with different roughness. One region corresponding to composition (1) has low roughness and the other region corresponding to composition (2) has high roughness.

Apparently, the growth of AlGaN with various Al/Ga ratios is significantly influenced by the silicon carbide sublayer quality in various substrate areas.

X-ray pattern of the AlGaN heterostructure (Sample № 3) formed on SiC/(111)Si substrate is shown in Fig. 2, *b, d*. Weak reflection at $2\theta \approx 36^\circ$ corresponds to a thin aluminum nitride sublayer formed directly on silicon carbide. The broadened reflection at $2\theta \approx 34.5{-}35^\circ$ may be indicative of the fact that there are $Al_xGa_{1-x}N$ interlayers with high aluminum content against the background of layers corresponding to the composition with Al/Ga = 0.5/0.5. The heterostructure of Sample № 4 predominantly consisted of the layers with composition close to $Al_{0.5}Ga_{0.5}N$, with sublayers enriched with aluminum atoms as in the previous case.

The analysis of formation of interlayers (or periodic AlGaN structure) observed before [24,25] shows that such structure is a result of composition self-organization and formation of a complex composite material that is apparently associated with periodic relaxation of mechanical stresses accumulated during heterostructure growth. It can be believed that the alteration of the composite material composition is accompanied with formation of heterojunctions and built-in space charge system; the latter shall severely affect the demonstration of dielectric and pyroelectric properties.

Pyroelectric response shapes of heterostructures (Samples № 2 and 4) at 1 Hz (*a, c*) and 1000 Hz (*b, d*) are shown in Fig. 3. The nature of pyroelectric responses of Samples № 1 and 3 corresponded to the response shape and amplitude typical of Samples № 2. The pyroelectric response measurements were obtained in the electric current recording mode using an operational amplifier.

The pyroelectric coefficient calculation carried out using the equation from [23] has shown that pyroelectric responses (pyroelectric coefficients „γ“) of AlGaN heterostructures (Samples № 1, 2 and 3) had a subtle difference from each other and the pyroelectric coefficients varied within $\gamma \sim (0.7{-}1) \cdot 10^{-10}$ C/cm^{2}K. The pyroelectric response from the heterostructure (Sample № 4) composed of thin AlGaN layers and thick AlN layers was significantly higher and showed $\gamma \sim 18 \cdot 10^{-10}$ C/cm^{2}K, i.e. virtually 20–25 times higher than that of multilayer AlGaN.

Extremely low pyroelectric coefficient values observed in different AlGaN structures grown in the polar axis [002] direction both on SiC/(111)Si and SiC/(110)Si substrates are probably associated with growth features of these structures. It can be expected that the growth of each next sublayer takes place when the polar axis orientation is changed to the opposite direction. In this case, the heat flux impact causes charge shifts in adjacent layers towards each other

and the recorded resultant pyroelectric current is a result of subtraction of the induced current of each sublayer, rather than of addition. A similar approach for multilayer nitride structures was used to explain significant reduction of pyroelectric coefficient in a three-layer aluminum nitride structure grown directly on SiC/(111)Si substrate [26]. As opposed to Samples № 1–3, one of the best pyroelectic coefficients achieved on epitaxial AlN layers was obtained in Sample № 4 due to the dominance of the aluminum nitride layer whose thickness was more than 90% of the heterostructure structure.

4. Conclusion

Thus, the pyroelectric properties of complex composite structures consisting of periodic $Al_xGa_{1-x}N$ layers with various composition that are perpendicular to the growth direction and were grown on hybrid SiC/Si(111) and SiC/Si(110) substrates by the CHE method. Hybrid SiC/Si(111) and SiC/Si(110) substrates were synthesized by a new matched atom substitution method. The pyroelectric coefficient measurements in these heterostructures have shown that their pyroelectric coefficients have close values of $\gamma \sim (0.7-1) \cdot 10^{-10}$ C/cm^{2}K regardless of the orientation of the initial Si substrate. It is shown that in order to increase the pyroelectric response, a AlN layer with a thickness greater than $1\,\mu$m shall be applied to $Al_xGa_{1-x}N$/SiC/Si surface. Is has been found that an additional AlN layer applied to the $Al_xGa_{1-x}N$/SiC/Si heterostructure surface resulted in formation of a new $AlN/Al_xGa_{1-x}N$/SiC/Si composite structure that has a pyroelectric coefficient of $\gamma \sim 18 \cdot 10^{-10}$ C/cm^{2}K that is unprecedented for AlN crystals and films.

Funding

The research was carried out as part of project No. 20-12-00193 of the Russian Science Foundation.

A part of the experimental studies was carried out using the equipment provided by the Center for the Collective Use of Scientific Equipment „Composition, Structure and Properties of Structural and Functional Materials“ National Research Center „Kurchatov Institute“— Central Research Institute of Structural Materials „Prometey“.

SiC-on-Si films were grown using the equipment of the Unique Scientific Unit „Physics, Chemistry, and Mechanics of Crystals and Thin Films“ (Institute for Problems in Mechanical Engineering of the Russian Academy of Sciences, St. Petersburg).

Conflict of interest

The authors declare that they have no conflict of interest.

References

[1] S. Nakamura, T. Mukai, M. Senoh. Appl. Phys. Lett. **64**, 1687 (1994).
[2] S. Guha, N.A. Bojarczuk. Appl. Phys. Lett. **72**, 415 (1998).
[3] M. Kneissl, Zh. Yang, M. Teepe, C. Knollenberg, O. Schmidt, P. Kiesel, N.M. Johnson, S. Schujman, L.J. Schowalter. J. Appl. Phys. **101**, 123103 (2007).
[4] S. Keller, C.S. Suh, Z. Chen, R. Chu, S. Rajan, N.A. Fichtenbaum, M. Furukawa, S.P. DenBaars, J.S. Speck, U.K. Mishra. J. Appl. Phys. **103**, 033708 (2008).
[5] P. Dong, J.-C. Yan, J.-X. Wang, Y. Zhang, C. Geng, T.-B. Wei, P.-P. Cong, Y.-U. Zhang, J.-P. Zeng, Y.-D. Tian, L. Sun, Q.F. Yan, J.-M. Li, S.-F. Fan, Z.-X. Qin. Appl. Phys. Lett. **102**, 241113 (2013).
[6] W. Guo, Z. Bryan, J.-Q. Xie, R. Kirste, S. Mita, I. Bryan, L. Hussey, M. Bobea, B. Haidet, M. Gerhold, R. Collazo, Z. Sitar. J. Appl. Phys. **115**, 103108 (2014).
[7] K. Lee, R. Page, V. Protasenko, L.J. Schowalter, M. Toita, H.G. Xing, D. Jena. Appl. Phys. Lett. **118**, 092101 (2021).
[8] S.A. Kukushkin, A.V. Osipov. Phys. Solid State **50**, *7*, 1238 (2008). DOI: 10.1134/S1063783408070081
[9] S.A. Kukushkin, A.V. Osipov. J. Phys. D **47**, *31*, 313001 (2014).
[10] S.A. Kukushkin, A.V. Osipov, N.A. Feoktistov. Phys. Solid State **56**, 1507 (2014). DOI: 10.1134/S1063783414080137
[11] V.N. Bessolov, Yu.V. Zhilyaev, E.V. Konenkova, L.M. Sorokin, N.A. Feoktistov, Sh.Sh. Sharofidinov, M.P. Shcheglov, S.A. Kukushkin, L.I. Mets, A.V. Osipov. Tech. Phys. Lett., **36**, *6*, 496 (2010) DOI: 10.1134/S1063785010060039
[12] V.N. Bessolov, Yu.V. Zhilyaev, E.V. Konenkova, L.M. Sorokin, N.A. Feoktistov, Sh.Sh. Sharofidinov, M.P. Shcheglov, S.A. Kukushkin, L.I. Mets, A.V. Osipov. J. Opt. Technol. **78**, 435 (2011). https://doi.org/10.1364/JOT.78.000435
[13] S.A. Kukushkin, Sh.Sh. Sharofidinov. Phys. Solid State **61**, 2342 (2019). DOI: 10.1134/S1063783419120254
[14] K. Fujito, Sh. Kubo, H. Nagaoka, T. Mochizuki, H. Namita, S. Nagao. J. Cryst. Growth **311**, *10*, 3011 (2009).
[15] J.A. Freitas, J.C. Culbertson, N.A. Mahadik, T. Sochacki, M. Iwinska, M.S. Bockowski. J. Cryst. Growth **456**, 113 (2016).
[16] P. Muralt. Rep. Prog. Phys. **64**, 1339 (2001).
[17] P. Muralt. J. Am. Ceram. Soc. **91**, *5*, 1385 (2008).
[18] M.S. Shur. Noise in devices and circuits III. Proc. SPIE, **5844**, 248 (2005).
[19] S.Yu. Davydov, O.V. Posrednik, FTT **58**, *4*, 630 (2019) (in Russian).
[20] L. Natta, V.M. Mastronardi, F. Guido, L. Algieri, S. Puce, F. Pisano, F. Rizzi, R. Pulli, A. Qualtieri, M. De Vittorio. Sci. Rep. **9**, 8392 (2019).
[21] O.N. Sergeeva, A.A. Bogomolov, A.V. Solnyshkin, N.V. Komarov, S.A. Kukushkin, D.M. Krasovitsky, A.L. Dudin, D.A. Kiselev, S.V. Ksenich, S.V. Senkevich, E.Yu. Kaptelov I.P. Pronin. Ferroelectrics **477**, 121 (2015).
[22] G.E. Stan, M. Botea, G.A. Boni, I. Pintilie, L. Pintilie. Appl. Surf. Sci. **353**, 1195 (2015).
[23] O.N. Sergeeva, A.V. Solnyshkin, D.A. Kiselev, T.S. Il'ina, S.A. Kukushkin, A.V. Osipov, Sh.Sh. Sharofidinov, E.Yu. Kaptelov, I.P. Pronin. Phys. Solid State **61**, 2386 (2019). DOI: 10.1134/S1063783419120485

[24] S.A. Kukushkin, Sh.Sh. Sharofidinov, A.V. Osipov, A.S. Grashchenko, A.V. Kandakov, E.V. Osipova, K.P. Kotlyar, E.V. Ubyivovk, Phys. Solid State **63**, 442 (2021). DOI: 10.1134/S1063783421030100
[25] A.V. Solnyshkin, O.N. Sergeeva, O.A. Shustova, Sh.Sh. Sharofidinov, M.V. Staritsyn, E.Yu. Kaptelov, S.A. Kukushkin, I.P. Pronin. Tech. Phys. Lett., **47**, *5*, 426 (2021). DOI: 10.1134/S1063785021050138
[26] O.A. Shustova, O.N. Sergeeva, A.V. Solnyshkin, I.T. Zezianov, E.Yu. Kaptelov, I.P. Pronin, Sh.Sh. Sharofudinov, S.A. Kukushkin. Ferroelectrics **591**, 121 (2022).